Athermal Fracture of Elastic Networks: How Rigidity Challenges the Unavoidable Size-Induced Brittleness

Simone Dussi,* Justin Tauber, and Jasper van der Gucht
Physical Chemistry and Soft Matter, Wageningen University, Stippeneng 4, 6708 WE, Wageningen, Netherlands

(Received 26 July 2019; published 10 January 2020)

By performing extensive simulations with unprecedentedly large system sizes, we unveil how rigidity influences the fracture of disordered materials. We observe the largest damage in networks with connectivity close to the isostatic point and when the rupture thresholds are small. However, irrespective of network and spring properties, a more brittle fracture is observed upon increasing system size. Differently from most of the fracture descriptors, the maximum stress drop, a proxy for brittleness, displays a universal nonmonotonic dependence on system size. Based on this uncommon trend it is possible to identify the characteristic system size L^* at which brittleness kicks in. The more the disorder in network connectivity or in spring thresholds, the larger L^*. Finally, we speculate how this size-induced brittleness is influenced by thermal fluctuations.

DOI: 10.1103/PhysRevLett.124.018002

Since the pioneering work of Griffith on crack nucleation in ordered materials with isolated defects [1], the last 30 years have witnessed a still-growing interest for fracture occurring in intrinsically disordered materials [2–9]. The fracture behavior of a material is intimately related to its microscopic structure, especially when thermal fluctuations are not relevant. How stress is (re)distributed during deformation and after bond-breaking events determines the material mechanical response. Abruptness is the hallmark of brittle fracture: the mechanical response of a brittle material subjected to an increasing strain deformation suddenly vanishes after reaching a peak. This is the macroscopic consequence of stress concentration in the system that induces bond-breaking events and triggers the nucleation of a crack that irremediably propagates throughout the system. For (more) ductile systems, such a catastrophic breaking event is absent or postponed much after the stress peak. As a consequence, the mechanical response of ductile materials persists after the peak.

Biopolymer networks, such as collagen, are ubiquitous examples of disordered structures, with a peculiarly low connectivity that places these materials below the isostatic point of mechanical stability [10]. At small deformation, these networks would not be rigid without their fiber bending stiffness, responsible for their small linear modulus. However, exactly because of their subisostaticity these materials show an extraordinary strain stiffening; i.e., their modulus increases by orders of magnitude when deformed above an onset strain. This mechanical response is a consequence of an athermal strain-driven rigidity transition: beyond the onset strain, the stretching of the bonds starts to control the network response and is sufficient to rigidify the system [11–19]. In fact, when deformed, these diluted elastic networks exhibit a very heterogeneous stress distribution with emerging force chains [20–24] [see Fig. 1(a)], similarly to deformed granular and porous materials [25–28]. The effects of these heterogeneous stresses on fracture have been only partially addressed.

It was recently argued that a continuous breakage and formation of force chains in subisostatic networks leads to a complete suppression of stress concentration, thereby

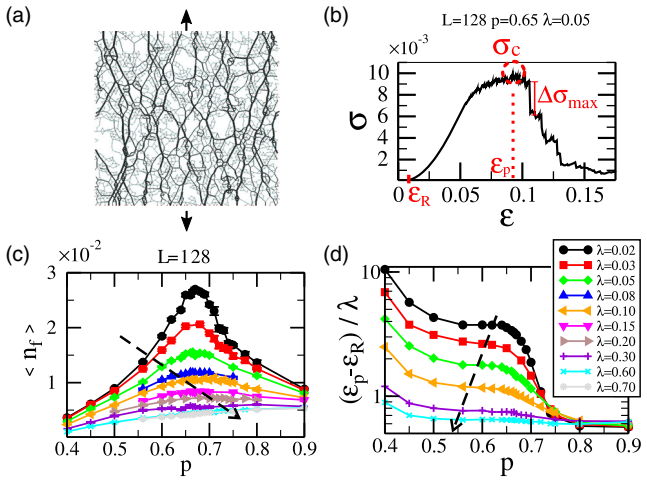

FIG. 1. Fracture depends on connectivity and thresholds. (a) When deforming diluted elastic networks, aligned sets of load-bearing bonds, called force chains, appear. Line thickness quantifies spring deformation. (b) Example of stress σ—strain ϵ curve and fracture descriptors. (c) Fraction of broken bonds at failure n_f and (d) *hidden length* exploited in the fracture process, as a function of the connectivity parameter p for different rupture threshold λ and fixed system size $L = 128$. Results are for 2D triangular networks.

preventing crack nucleation at all length scales [23]. This conclusion clashes with a recent theory (that does not explicitly account for material rigidity) that predicts crack nucleation for any disordered system approaching the thermodynamic limit (infinite system size) [8]. This raises the question whether sparse elastic networks show fracture behavior that differs qualitatively from that of other disordered materials. Evidence based on simulations of moderate system size [23,29] and fracture experiments on small meta-materials [29–31] shows that rigidity cannot be neglected if one wishes to understand fracture in these materials. More generally, despite recent progress [28,32–36], a clear link between network structure and fracture is still missing, even for a cornerstone such as the central-force spring network model. In this Letter, by fully characterizing the fracture of such a model, we aim to demonstrate whether the tuning of rigidity can actually suppress crack nucleation or not.

We perform (off-lattice) simulations of diluted spring networks with different connectivity, rupture thresholds, topologies, and unprecedentedly large system sizes. Here, we focus on triangular networks made of $L \times L$ nodes in which a fraction $1 - p$ of the bonds is removed. Results from other topologies are reported in the Supplemental Material [37]. All bonds are harmonic springs with unit stiffness and unit rest length. A bond breaks irreversibly when its deformation exceeds the rupture threshold λ (same for all springs). We deform the networks uniaxially in the y direction under athermal and quasistatic loading conditions, by applying small strain steps and using the FIRE algorithm [38] to minimize the energy in between strain steps and breaking events. We characterize the network response by measuring the stress σ, defined as the yy component of the virial stress tensor, as a function of the (engineering) strain $\epsilon = (L_y - L_y^{(0)})/L_y^{(0)}$, where L_y and $L_y^{(0)}$ are the system dimension during and before the deformation, respectively. We identify the strain ϵ_R at which the network rigidifies (i.e., when σ exceeds the numerical noise), the maximum stress σ_c and its associated strain value ϵ_p, and the maximum stress drop $\Delta\sigma_{\max}$, as illustrated in Fig. 1(b). Furthermore, we calculate the fraction of broken bonds at final failure (defined when the network is broken in two parts) $n_f = N_f/N_{\text{in}}$, with N_f the number of broken bonds at failure and N_{in} the number of intact bonds at rest. Quantities are expressed in reduced units and averaged over many configurations (see Supplemental Material [37] for details).

In Fig. 1, we show results at fixed system size $L = 128$. In panel (c), we observe for small λ a nonmonotonic dependence of n_f on the network connectivity, with a maximum around the isostatic point [10] ($p_{\text{iso}} \simeq 0.66$), consistently with Ref. [23]. Approaching the limit of a fully connected network ($p = 1$), the number of broken bonds drastically diminishes, as expected for a more homogeneous material that typically breaks in a brittle fashion via crack nucleation at the weakest spot followed by a localized propagation involving only few bonds. Also at the other extreme of the connectivity range, close to the geometric percolation limit $p_g \simeq 0.347$, only few bonds are needed to break the already loosely connected networks. Interestingly, when increasing λ, that is the strength of the individual springs, n_f decreases for all p and the maximum around p_{iso} disappears. Therefore, a general gradual transition to a more localized type of fracture is observed when the breaking process starts at larger deformation (larger λ) that corresponds to a larger system response (higher stress and modulus). This implies that a more rigid system breaks in a more brittle fashion. To further quantify the role of the network architecture on the fracture process, we plot in Fig. 1(d) the hidden length emerging during the deformation, defined as the strain interval $\epsilon_p - \epsilon_R$ in which the (rigidified) network reaches the stress peak, normalized by the stretchability of the individual elements λ. For small λ, we observe that $(\epsilon_p - \epsilon_R)/\lambda > 1$ for networks with $p \lessapprox p_{\text{iso}}$, meaning that they can be stretched significantly more than their elements before network fracture occurs. This is a macroscopic consequence of the underlying complex and heterogeneous stress (re)distribution during the deformation, involving nonaffine displacements and formation or breakage of force chains [16,20,23,39]. By contrast, for large p and/or for large λ the hidden length is less than unity, indicating that significant stress concentration occurs before exploiting all the possible bonds stretchability. From our analysis (other quantities are shown in the Supplemental Material [37]) we can evidently conclude that the fracture process can be tuned by varying p and λ from brittle (abrupt postpeak response, fracture is localized in space and time) to more ductile (more continuous postpeak response, and damage is larger and more diffuse) when $L = 128$. We confirmed the universality of the observed behavior by simulating two- and three-dimensional diluted networks with different topologies (see Supplemental Material [37]).

Next, we study the effect of system size, known to be crucial in fracture [6,21,40,41], to understand if the locally inhomogeneous stress (re)distribution still has macroscopic implications in larger systems. First, we consider the total number of broken bonds at failure N_f as a function of the system size L and extract the damage fractal dimension d_f by fitting $N_f \sim L^{d_f}$, as shown in Fig. 2(a) for $p = 0.65$, $\lambda = 0.03$. In Fig. 2(b), we plot d_f for several connectivities and thresholds. We observe that d_f is larger close to the isostatic point and for small λ. When increasing λ and/or moving away from p_{iso}, d_f gradually decreases and approaches the expected $d_f = 1$ for brittle fracture where a crack propagates almost in a straight line, and therefore the number of broken bonds scales linearly with system size. The upper bound of $d_f = 2$ for which damage is

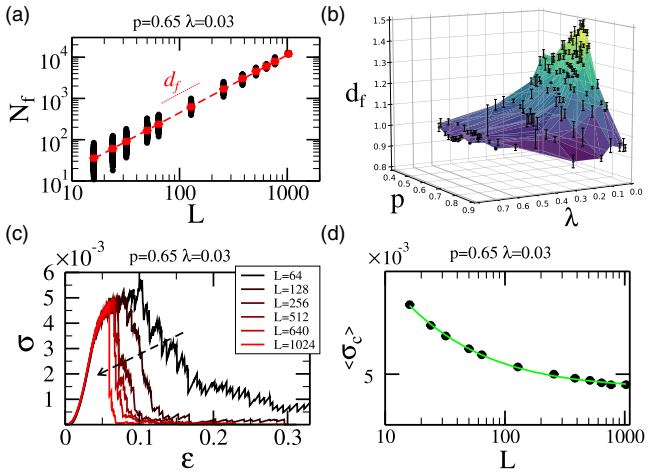

FIG. 2. The role of system size. (a) Size scaling of number of broken bonds N_f for triangular networks with $p = 0.65$, $\lambda = 0.03$. Black circles indicate single-run values, red squares are averages, and the dashed line is the power-law fit used to extract d_f. (b) Damage fractal dimension d_f as a function of p and λ. (c) Single-run stress-strain curve for increasing system size L, showing that response is abrupt for large L. (d) Size scaling of the maximum stress σ_c (log-log plot). Symbols correspond to averages and the line is the best fit. Data follow a power-law decay. Results are for 2D triangular networks.

completely delocalized [7] might be expected only when $\lambda \to 0$. Second, in Fig. 2(c), we show the stress-strain curve for different system sizes of networks close to the isostatic point and with small λ. Despite the fact that d_f is maximal for these networks, we observe that their response becomes evidently more brittle for larger L. We also note that the maximum stress σ_c, as exemplarily shown in Fig. 2(d), decreases upon increasing system size, as commonly observed in fracture studies, towards a limiting value $\sigma_c^{(\infty)} \neq 0$ that depends on p and λ. In passing, we note that our data suggest that σ_c decays following a power law, therefore in a qualitatively different way compared to the scalar models that have been extensively used so far to describe fracture of disordered materials [3,42,43] (see also Supplemental Material [37]). Finally, we quantify the fracture abruptness by looking at the maximum stress drop $\Delta\sigma_{\max}$. Strikingly, instead of a conventional monotonic decay with increasing system size, we observe a nonmonotonic trend, as shown in Fig. 3(a), for networks close to p_{iso} and with $\lambda = 0.03$. For small L, $\Delta\sigma_{\max}$ decreases upon increasing system size. For a second-order transition, for which the system response vanishes continuously, we would expect $\Delta\sigma_{\max} \to 0$ for $L \to \infty$. However, the decrease in abruptness stops around $L \simeq 128$. At the same time, the increase of $\Delta\sigma_{\max}$ observed for networks containing up to a few million bonds ($L = 1024$) cannot continue for even larger (computationally inaccessible) system sizes since $\Delta\sigma_{\max} \leq \sigma_c$ must hold and we found that σ_c decreases with increasing L. Indeed, when simulating networks with $p = 0.75$ and $\lambda = 0.10$, as shown in Fig. 3(b) (solid lines), we observe a slower increase of $\Delta\sigma_{\max}$ when approaching the limiting value of σ_c. A third region where $\Delta\sigma_{\max} \sim \sigma_c$, indicative of brittle fracture, becomes clear in panel (c) where we show results for $p = 0.90$ and $\lambda = 0.30$. Therefore, there must exist a relation between the rigidity-controlled damage, quantified via d_f, and the system size intervals corresponding to the three fracture regimes. Indeed, when plotting in panel (d) the abruptness for simulations at fixed $p = 0.65$ and increasing λ, i.e., decreasing the associated d_f, it seems that each individual curve represents a different part of a universal response. In fact, we were able to manually rescale and collapse the data onto a master curve (see Supplemental Material [37]), schematically depicted in panel (e). At present, we are unable to provide an analytical expression for the scaling function. Nevertheless, the transitions between the three regimes must reflect the underlying stress (re)distribution processes. For small L, the mechanical response is dominated by breakage and reformation of force chains and $\Delta\sigma_{\max}$ initially decreases when more force chains are present upon increasing L. However, above a certain length scale L^* (either the maximum or the minimum of the curve) force chains are ineffective in avoiding stress concentration and brittle fracture is observed. Both network structure and spring properties control these transitions. To further prove this statement, we consider additional disorder by drawing random thresholds from a uniform distribution. In Fig. 3(b), we show results for networks with the same $p = 0.75$ and average $\langle\lambda\rangle = 0.10$, but with individual spring thresholds λ_i drawn from two different intervals (as indicated in the legend) and when no disorder is present ($\lambda_i = 0.10\ \forall\ i$). We observe that the minimum in $\Delta\sigma_{\max}$ shifts to larger L when the threshold distribution is broader. In short, the larger the (connectivity or threshold) disorder, the larger the system size L^* at which brittleness kicks in. We find that the nonmonotonic size scaling of fracture abruptness is universal, irrespective of network topology or technical details regarding boundary conditions and simulation protocols (see Supplemental Material [37]).

Our study shows that the fracture process of truly large ($L > L^*$) elastic networks is always dominated by stress concentration leading to unavoidably abrupt fracture when the critical deformation (ϵ_p, σ_c) is reached. In contrast with the conclusions of Ref. [23], we have shown that also subisostatic networks break via crack nucleation when sufficiently large. Our results are consistent with the idea of crack nucleation as limiting fracture behavior for disordered materials [8]. However, differently from the finite-size criticality of Ref. [8] that manifests itself as a smooth crossover in exponents associated to (avalanche or crack size) distributions, the size-induced brittleness studied here gives rise to a nonmonotonic size dependence of $\Delta\sigma_{\max}$. The extreme point(s) of such a trend can be used to

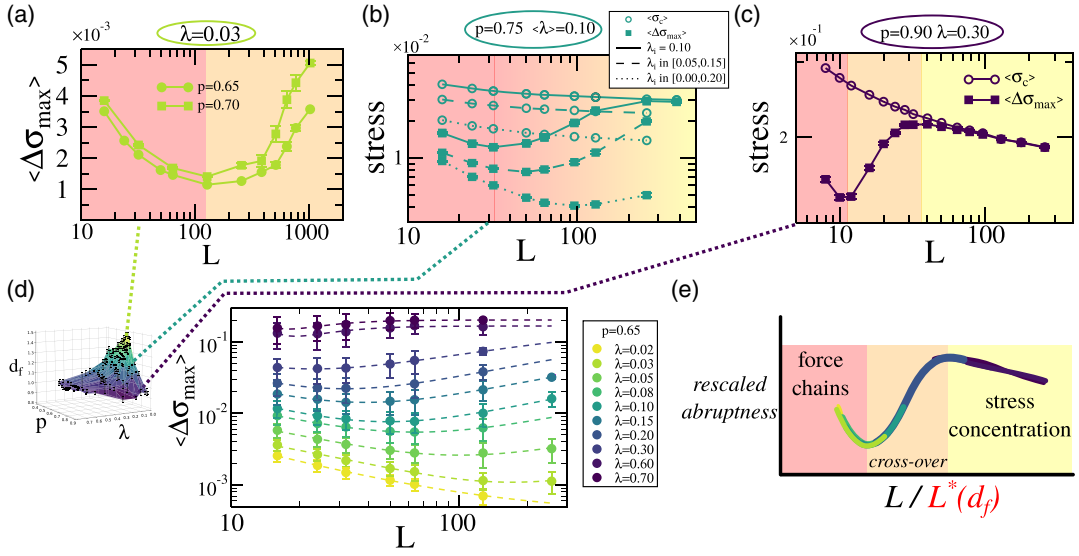

FIG. 3. Regimes based on fracture abruptness. (a) Size scaling of fracture abruptness $\Delta\sigma_{\max}$ for networks close to the isostatic point with small λ. A minimum in the trend is evident. (b) Size scaling of maximum stress (empty circles) and fracture abruptness (filled squares) for diluted networks ($p = 0.75$) with all springs with same $\lambda_i = 0.10$ (solid lines), and with additional disorder in the spring thresholds λ_i uniformly distributed in the two intervals indicated in the legend (dashed and dotted lines). The additional threshold disorder shifts the minimum to larger L. (c) For $p = 0.90$ and $\lambda = 0.30$, a third region is probed for large L where the abruptness scales as the maximum stress. (d) Size scaling of abruptness close to the isostatic point for different λ, color coded with the associated damage fractal dimension d_f (inset). (e) Universal trend for rescaled abruptness (see also Supplemental Material [37]): at small L force chains dominate the mechanical response but beyond L^* stress concentration leading to abrupt fracture is unavoidable. Results are for 2D triangular networks.

define a characteristic size L^* corresponding to the transition from ductile to brittle crack nucleation. Despite the abrupt nature of fracture, we have also shown that the damage can be delocalized in space due to the inhomogeneous network structure. In fact, the damage zone spans the entire system with a distinct fractal dimension $d_f > 1$, as illustrated in the left postmortem snapshot of Fig. 4. This is reminiscent of some fracture modes investigated using fiber bundle models [44], where however the range of stress redistribution is an imposed parameter instead of an emerging structure property.

Finally, we conclude this Letter by showing an unexpected dependence on the tolerance parameter F_{RMS} used in the energy minimization protocol employed in our simulations. [37,38] F_{RMS} is the maximum force per node allowed in the system after a deformation step or breaking event. Typically, F_{RMS} is chosen small enough to ensure that the system is in its energy minimum, or equivalently in mechanical equilibrium, and therefore the simulation is in the athermal (energy-dominated) limit. In Fig. 4, we plot the size scaling of N_f for different F_{RMS} and we observe that for the huge system sizes investigated here a great number of additional bonds are broken when a larger F_{RMS} is used. Correspondingly, a more ductile response is obtained due to the formation of multiple macrocracks. Therefore, we remark that (i) to reach the athermal limit when a large d_f is expected, an increasingly smaller F_{RMS} might be needed to simulate increasingly larger networks, (ii) since using a larger F_{RMS} corresponds to push the system close but not at its energy minimum, F_{RMS} could be a proxy for temperature. According to this interpretation, thermal fluctuations would couple with large rigidity fluctuations around the isostatic point, giving rise to ductile behavior even for large system sizes. Further studies are needed to confirm the latter intriguing speculation.

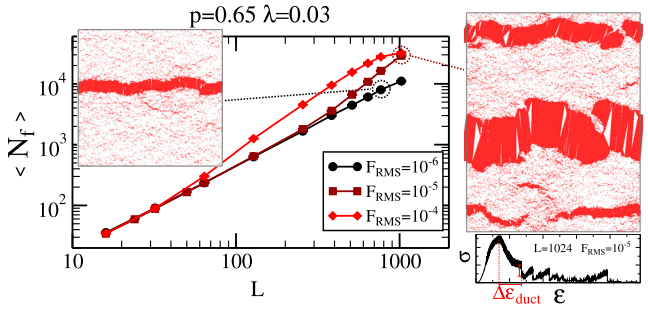

FIG. 4. Athermal limit and macroscopic cracks. Main graph: Size scaling of broken bonds for simulations performed with different energy minimization tolerance F_{RMS}. Larger L requires lower F_{RMS} to perform simulations in the athermal limit, where fracture occurs due to a single macrocrack (see postmortem snapshot on the left, where only broken bonds are shown). For larger F_{RMS} and huge system sizes, multiple macrocracks are observed (right snapshot) and the network response shows a large ductile interval $\Delta\epsilon_{\mathrm{duct}}$ (bottom right).

In summary, our results demonstrate that athermal networks unavoidably break in a brittle fashion when approaching the thermodynamic limit, i.e., when increasing the system size beyond a characteristic length scale L^*. We have shown that L^* can be controlled by tuning individual elements or their assembly, with larger disorder increasing L^*. Furthermore, we found that the fractal dimension of the damage zone d_f is coupled with L^* and can be very large close to the isostatic point [23,29], which can be interpreted as a critical point for fracture. These considerations are relevant not only for metamaterials (for which L is small and λ or the network geometry can be easily tuned) but also for biological samples, since they are also often far from the thermodynamic limit. For example, biopolymer networks between two cells should have sizes well below L^* to prevent catastrophic failure, and even reconstituted collagen networks inside a rheometer have shown size-dependent fracture behavior [45].

This work is part of the SOFTBREAK project funded by the European Research Council (ERC Consolidator Grant). S. D. thanks Xiaoming Mao for informative correspondence. We thank Jessi van der Hoeven for a critical reading of the manuscript.

*simone.dussi@wur.nl

[1] A. A. Griffith, Phil. Trans. R. Soc. A **221**, 163 (1921).
[2] M. Sahimi and J. D. Goddard, Phys. Rev. B **33**, 7848 (1986).
[3] P. M. Duxbury, P. L. Leath, and P. D. Beale, Phys. Rev. B **36**, 367 (1987).
[4] B. Kahng, G. G. Batrouni, S. Redner, L. de Arcangelis, and H. J. Herrmann, Phys. Rev. B **37**, 7625 (1988).
[5] S. Zapperi, P. Ray, H. E. Stanley, and A. Vespignani, Phys. Rev. E **78**, 1408 (1997).
[6] M. J. Alava, P. K. V. V. Nukala, and S. Zapperi, Adv. Phys. **55**, 349 (2006).
[7] A. A. Moreira, C. L. N. Oliveira, A. Hansen, N. A. M. Araújo, H. J. Herrmann, and J. S. Andrade, Jr., Phys. Rev. Lett. **109**, 255701 (2012).
[8] A. Shekhawat, S. Zapperi, and J. P. Sethna, Phys. Rev. Lett. **110**, 185505 (2013).
[9] H. J. Herrmann and S. Roux, *Statistical Models for the Fracture of Disordered Media* (Elsevier, North Holland, Amsterdam, 1990).
[10] J. C. Maxwell, Philos. Mag. **27**, 294 (1864).
[11] P. R. Onck, T. Koeman, T. van Dillen, and E. van der Giessen, Phys. Rev. Lett. **95**, 178102 (2005).
[12] M. Wyart, H. Liang, A. Kabla, and L. Mahadevan, Phys. Rev. Lett. **101**, 215501 (2008).
[13] A. J. Licup, S. Münster, A. Sharma, M. Sheinman, L. M. Jawerth, B. Fabry, D. A. Weitz, and F. C. MacKintosh, Proc. Natl. Acad. Sci. U.S.A. **112**, 9573 (2015).
[14] A. Sharma, A. J. Licup, K. A. Jansen, R. Rens, M. Sheinman, G. H. Koenderink, and F. C. MacKintosh, Nat. Phys. **12**, 584 (2016).
[15] J. Feng, H. Levine, X. Mao, and L. M. Sander, Soft Matter **12**, 1419 (2016).
[16] C. P. Broedersz and F. C. MacKintosh, Rev. Mod. Phys. **86**, 995 (2014).
[17] M. F. J. Vermeulen, A. Bose, C. Storm, and W. G. Ellenbroek, Phys. Rev. E **96**, 053003 (2017).
[18] F. Burla, J. Tauber, S. Dussi, J. van der Gucht, and G. Koenderink, Nat. Phys. **15**, 549 (2019).
[19] J. L. Shivers, S. Arzash, A. Sharma, and F. C. MacKintosh, Phys. Rev. Lett. **122**, 188003 (2019).
[20] C. Heussinger and E. Frey, Eur. Phys. J. E **24**, 47 (2007).
[21] R. C. Arevalo, P. Kumar, J. S. Urbach, and D. L. Blair, PLoS One **10**, e0118021 (2015).
[22] L. Liang, C. Jones, S. Chen, B. Sun, and Y. Jiao, Phys. Biol. **13**, 066001 (2016).
[23] L. Zhang, D. Z. Rocklin, L. M. Sander, and X. Mao, Phys. Rev. Mater. **1**, 052602(R) (2017).
[24] J. L. Shivers, J. Feng, A. Sharma, and F. C. MacKintosh, Soft Matter **15**, 1666 (2019).
[25] M. E. Cates, J. P. Wittmer, J.-P. Bouchaud, and P. Claudin, Phys. Rev. Lett. **81**, 1841 (1998).
[26] C. S. O'Hern, S. A. Langer, A. J. Liu, and S. R. Nagel, Phys. Rev. Lett. **86**, 111 (2001).
[27] T. S. Majmudar and R. P. Behringer, Nature (London) **435**, 1079 (2005).
[28] H. Laubie, F. Radjai, R. Pellenq, and F.-J. Ulm, Phys. Rev. Lett. **119**, 075501 (2017).
[29] M. M. Driscoll, B. G. Chen, T. H. Beuman, S. Ulrich, S. R. Nagel, and V. Vitelli, Proc. Natl. Acad. Sci. U.S.A. **113**, 10813 (2016).
[30] E. Berthier, J. E. Kollmer, S. E. Henkes, K. Liu, J. M. Schwarz, and K. E. Daniels, Phys. Rev. Mater. **3**, 075602 (2019).
[31] Z. Qin, G. S. Jung, M. J. Kang, and M. J. Buehler, Sci. Adv. **3**, e1601536 (2017).
[32] W. G. Ellenbroek, V. F. Hagh, A. Kumar, M. F. Thorpe, and M. van Hecke, Phys. Rev. Lett. **114**, 135501 (2015).
[33] I. Malakhovsky and M. A. J. Michels, Phys. Rev. B **74**, 014206 (2006).
[34] L. Girard, J. Weiss, and D. Amitrano, Phys. Rev. Lett. **108**, 225502 (2012).
[35] M. Bouzid, J. Colombo, L. V. Barbosa, and E. D. Gado, Nat. Commun. **8**, 15846 (2017).
[36] S. Bonfanti, E. E. Ferrero, A. L. Sellerio, R. Guerra, and S. Zapperi, Nano Lett. **18**, 4100 (2018).
[37] See Supplemental Material at http://link.aps.org/supplemental/10.1103/PhysRevLett.124.018002 for details on simulation methods and additional results.
[38] E. Bitzek, P. Koskinen, F. Gähler, M. Moseler, and P. Gumbsch, Phys. Rev. Lett. **97**, 170201 (2006).
[39] W. G. Ellenbroek, Z. Zeravcic, W. van Saarloos, and M. van Hecke, Europhys. Lett. **87**, 34004 (2009).
[40] M. J. Alava, P. K. V. V. Nukala, and S. Zapperi, Phys. Rev. Lett. **100**, 055502 (2008).
[41] A. Taloni, M. Vodret, G. Costantini, and S. Zapperi, Nat. Rev. Mater. **3**, 211 (2018).
[42] C. Manzato, A. Shekhawat, P. K. V. V. Nukala, M. J. Alava, J. P. Sethna, and S. Zapperi, Phys. Rev. Lett. **108**, 065504 (2012).
[43] S. Roy, Phys. Rev. E **96**, 042142 (2017).
[44] S. Roy, S. Biwas, and P. Ray, Phys. Rev. E **96**, 063003 (2017).
[45] R. C. Arevalo, J. S. Urbach, and D. L. Blair, Biophys. J. **99**, L65 (2010).